Microfluidic preparation and in vitro evaluation of iRGD-functionalized solid lipid nanoparticles for targeted delivery of paclitaxel to tumor cells

Arduino, Ilaria

2021-12-15

Arduino , I , Liu , Z , Iacobazzi , R M , Lopedota , A A , Lopalco , A , Cutrignelli , A , Laquintana , V , Porcelli , L , Azzariti , A , Franco , M , Santos , H A & Denora , N 2021 , ' Microfluidic preparation and in vitro evaluation of iRGD-functionalized solid lipid nanoparticles for targeted delivery of paclitaxel to tumor cells ' , International Journal of Pharmaceutics , vol. 610 , 121246 . https://doi.org/10.1016/j.ijpharm.2021.121246

http://hdl.handle.net/10138/350334
https://doi.org/10.1016/j.ijpharm.2021.121246

International Journal of Pharmaceutics 610 (2021) 121246

Contents lists available at ScienceDirect

International Journal of Pharmaceutics

journal homepage: www.elsevier.com/locate/ijpharm

Microfluidic preparation and *in vitro* evaluation of iRGD-functionalized solid lipid nanoparticles for targeted delivery of paclitaxel to tumor cells

Ilaria Arduino [a,b], Zehua Liu [b], Rosa Maria Iacobazzi [c], Angela Assunta Lopedota [a], Antonio Lopalco [a], Annalisa Cutrignelli [a], Valentino Laquintana [a], Letizia Porcelli [c], Amalia Azzariti [c], Massimo Franco [a], Hélder A. Santos [b,d,*], Nunzio Denora [a,*]

[a] Department of Pharmacy – Pharmaceutical Sciences, University of Bari "Aldo Moro", Orabona St. 4, 70125 Bari, Italy
[b] Drug Research Program, Division of Pharmaceutical Chemistry and Technology, Faculty of Pharmacy, University of Helsinki, FI-00014 Helsinki, Finland
[c] Laboratory of Experimental Pharmacology, IRCCS IstitutoTumori "Giovanni Paolo II", O. Flacco St., 70124 Bari, Italy
[d] Department of Biomedical Engineering, University of Groningen / University Medical Center Groningen and W.J. Kolff Institute for Biomedical Engineering and Materials Science, Ant. Deusinglaan 1, 9713 AV Groningen, The Netherlands

ARTICLE INFO

Keywords:
Solid lipid nanoparticles
Microfluidics
iRGD peptide
3D cell culture
Targeted drug delivery
Tumor cell

ABSTRACT

Solid lipid nanoparticles (SLNs) can combine the advantages of different colloidal carriers and prevent some of their disadvantages. The production of nanoparticles by means of microfluidics represents a successful platform for industrial scale-up of nanoparticle manufacture in a reproducible way. The realisation of a microfluidic technique to obtain SLNs in a continuous and reproducible manner encouraged us to create surface functionalised SLNs for targeted drug release using the same procedure. A tumor homing peptide, iRGD, owning a cryptic C-end Rule (CendR) motif is responsible for neuropilin-1 (NRP-1) binding and for triggering extravasation and tumor penetration of the peptide. In this study, the Paclitaxel loaded-SLNs produced by microfluidics were functionalized with the iRGD peptide. The SLNs proved to be stable in aqueous medium andwere characterized by a Z-average under 150 nm, a polydispersity index below 0.2, a zeta-potential between −20 and −35 mV and a drug encapsulation efficiency around 40%. Moreover, *in vitro* cytotoxic effects and cellular uptake have been assessed using 2D and 3D tumour models of U87 glioblastoma cell lines. Overall, these results demonstrate that the surface functionalization of SLNs with iRGD allow better cellular uptake and cytotoxicity ability.

1. Introduction

Solid lipid nanoparticles (SLNs) are very interesting colloidal systems that have been studied for almost twenty years (Paliwal et al. 2020). Like other nanoparticle systems, SLNs provide drug protection from degradation, sustained release and target-dependent biodistribution, but providing greater stability and more tolerability compared to other lipid formulations and polymeric systems (Arduino et al. 2021). In fact, the use of solid lipids in the preparation of SLNs greatly reduces the mobility of the drug loaded into the lipid matrix and protects it from clearance by the reticuloendothelial system (Becker Peres et al. 2016). Furthermore, their surface is easily modified for improving the circulation time in the blood stream and/or directing them to a specific target.

However, conventional methods to produce nanoparticles, and in this specific case SLNs, lead to the formation of nanoparticle systems with a wide size distribution and an evident batch-to-batch variability linked to the loss of control over the experimental variables (Arduino et al. 2021). For these reasons, an industrial scale-up to produce nanoparticles represents a challenge.

In recent years, microfluidics, an emerging technology enabling the manipulation of fluid (in nanoliters scale) in micrometer channels, has attracted a lot of interest in biomedical and pharmaceutical fields because it can be used to produce nano/micro-particles in a continuous process (Costa et al. 2020; Costa et al. 2021; Hussain et al. 2020; Liu et al. (2017a); Liu et al. 2020). Microfluidics offers several advantages, including high batch-to-batch reproducibility, controlled manipulation of process parameters, thus providing the optimization and tunability of nanoparticles properties, including drugs encapsulation efficiency and monodispersity of batches (Martins et al. 2019). Polydimethylsiloxane (PDMS), glass and silica, are the common material used on the

* Corresponding authors at: Drug Research Program, Division of Pharmaceutical Chemistry and Technology, Faculty of Pharmacy, University of Helsinki, FI-00014 Helsinki, Finland (H.A. Santos). Department of Pharmacy – Pharmaceutical Sciences, University of Bari "Aldo Moro", Orabona St. 4, I-70125 Bari, Italy (N. Denora).
E-mail addresses: helder.santos@helsinki.fi (H.A. Santos), nunzio.denora@uniba.it (N. Denora).

https://doi.org/10.1016/j.ijpharm.2021.121246
Received 9 July 2021; Received in revised form 13 October 2021; Accepted 25 October 2021
Available online 28 October 2021

manufacturing of microfluidic devices. Among these different materials, glass is certainly the most suitable because it is cheap, inert towards organic solvents and it is easier to manufacture devices (Arduino et al. 2021); (Liu et al. (2017b)); (Martins et al. 2018); (Tahir et al. 2020).

Recently, we have developed the first set-up, known in literature, to produce SLNs by microfluidics (Arduino et al. 2021). We previously described the production of SLNs using glass-capillary microfluidic device through a systematic optimization process, opening a new avenue for the future standardization and scale-up of the production of such nanosystems. The achievement of a continuous and reproducible microfluidic method for the production of SLNs, prompted us to develop surface functionalized SLNs as targeted drug delivery system by using the same technique. SLNs can accumulate at tumour sites through the effect of enhanced permeability and retention (EPR) (Zheng et al. 2014), despite this, the design and microfluidics preparation of SLNs that could remain in blood circulation for longer time, also exploiting an active targeting to tumour sites is a very important challenge. The presence of polyethyleneglycol (PEG) molecules on the nanoparticle surface enable prolonged circulation time, while the functionalization of their surface with specific targeting moieties can improve the tumour selectivity and therapeutic efficacy of the nanoparticle system in many solid tumours (Zheng et al. 2014).

Integrin receptors are cation-dependent heterodimeric cell adhesion molecules which play an important role in cell adhesion, cell signalling and angiogenesis. Overexpression of the $\alpha_v\beta_3$ integrin receptor has been widely observed in many forms of solid tumors (Garanti et al. (2020)). Specifically, the internalizing RGD peptide (iRGD, CRGDRGPDC) is a 9-aminoacid cyclic peptide that has a special structure, including a vascular homing motif RGD, a protease recognition site and a tumour cell targeting motif CendR (Lu et al. 2020; Sugahara et al. 2009). The iRGD peptide homes to tumours by acting in different stages. Initially, it binds to integrin $\alpha_v\beta_3$, which are expressed more on tumor cells and endothelial cells of tumour vessels (Liu et al. (2017c); Ruoslahti and Pierschbacher 1987), then a tumor-derivated protease cleavage exposes the CendR motif that is a binding site for neuropilin-1 NRP-1. NRP-1 binding leads to trigger endocytic transcytosis and *trans*-tissue transport pathway that can assist drug and nanoparticle delivery, increasing transcytosis efficiency and penetration level in solid tumors (Liu et al. (2017c); Lu et al. 2020; Sugahara et al. 2010).

In this work, iRGD-functionalized SLNs (iRGD-SLN) and non-functionalized SLNs were developed by microfluidic technique. Paclitaxel (PTX), chosen as a model antitumor drug, was encapsulated within the produced SLNs. The iRGD-SLN system aimed to improve the anticancer potential of PTX by providing its selective delivery to cancer cells and increased accumulation and penetration into tumor site. SLNs were firstly characterized for their size and size distribution, drug encapsulation efficiency and drug release profile. Then, *in vitro* cell viability studies were conducted on human glioblastoma U87-MG cells overexpressing $\alpha_v\beta_3$ integrin receptor, in order to demonstrate the better efficacy of the PTX formulated in a targeted NPs system (iRGD-SLN-PTX) respect to PTX used as such. Moreover, the internalization studies of the targeted iRGD-SLN were conducted both in 2D and 3D *in vitro* models of human glioblastoma U87-MG cells by means of flow cytometric analysis and fluorescence imaging.

2. Materials and methods

2.1. Materials

All chemicals were of the highest purity available and were used as received without further purification or distillation.1,2-distearoyl-*sn*-glycero-3-phosphoethanolamine-N-[maleimide(polyethylene glycol)-2000] (ammonium salt) (DSPE-PEG-maleimide) was purchased from Avanti Polar Lipids. Cetyl palmitate was purchased from Farmalabor. Paclitaxel (PTX), Pluronic F68 and Tween 80 were purchased from Sigma Aldrich. All solvents used were of analytical grade and purchased from Aldrich. The iRGD (CCRGDKGPDC) was purchased from GenicBio. iRGD with a fluorescein isothiocyanate (FITC) was acquired from United BioSystem Inc. Bodipy alkyne dye (BDP) was acquired from Lumiprobe GmbH (Germany). All aqueous solutions were prepared using water obtained from a Milli-Q gradient A-10 system (Millipore, 18.2 MΩ•cm, organic carbon content $\geq$ 4 μg/L.Dulbecco's Modified Eagle's medium (DMEM), heat inactivated fetal bovine serum (FBS), L-glutamine (200 mM), non-essential amino acids (NEAA), penicillin (100 IU/mL), streptomycin (100 mg/mL) and trypsin (2.5%) were acquired from HyClone Waltham, USA. Phosphate buffer saline (10XPBS) and Hank's balanced salt solution (10 × HBSS) were purchased from Hyclone. Disposable culture flasks and Petri dishes were from Corning (Glassworks).

2.2. Preparation of glass capillary microfluidic chip

The microfluidic devices were assembled from borosilicate glass capillaries and glass rods. One end of the cylindrical glass capillary (World Precision Instruments, Inc.), with inner and outer diameters of 580 and 1000 μm, respectively, was tapered using a micropipette puller (P-97, Sutter Instrument Co., USA) to a diameter of 20 μm; this diameter was further enlarged to approximately 80 μm by using sandpaper (RHYNOWET P-2500, Indasa, USA). This cylindrical tapered capillary was inserted and coaxially aligned into the left end of the cylindrical capillary with inner dimension of 1100 μm (Vitrocom, USA) and a three-port valve is connected after the device (Arduino et al. 2021). Two miscible (functioning as outer and inner phase for nanoparticle production) liquids were injected separately into the microfluidic device through polyethylene tubes attached to syringes at constant flow rates, and the air was introduced to the solution through the three-port valve to further enhance the mixing efficiency. The flow rate of the different liquids was controlled by pumps (PHD 2000, Harvard Apparatus, USA). During the production of SLNs, it was fundamental to keep the temperature above 60 °C. In this regard, a supporting heating facility was designed and constructed by wrapping the lipid containing syringe with electric wire, which connected with a pressure regulator; the temperature of the electric wire wrapped syringe was controlled by altering the voltage, and the temperature was set to 60 °C. The microfluidic chip was immersed in water containing heating bath, and the temperature was also maintained at 60 °C.

2.3. Preparation of solid lipid nanoparticles by microfluidic technique

The SLNs were prepared by nanoprecipitation in a glass capillary microfluidics device (Arduino et al. 2021). The co-flow geometry is the main geometry for producing nanoparticles. In co-flow geometry, the fluids of the inner and the outer flow in parallel streams. The organic phase consisted of a mixture of 10 mg/mL of Cetil Palmitate and 3 mg/mL of DSPE-PEG-maleimide, containing 0.75 mg/mL of PTX. The aqueous phase consisted of 2% (w/v) of Pluronic F68.The organic and aqueous phase corresponded to the inner and outer fluid, respectively. With the usage of two microfluidics pumps, we set the flow rate of the inner (10 mL/min) and the outer solution (50 mL/min) and we kept the flow-rate constant. The liquids flowed from their respective syringes into the devices through tiny tubes. To remove the surfactant and non-encapsulated drug, the produced SLNs were carefully purified using centrifugal concentrators (Centrifugal Filter Units-Amicon Ultra 100 k) by ultrapure water at 4 °C, 3500 rpm for 15 min (5 times). Finally, the purified SLNs were stored at 4 °C.

2.4. Functionalization of solid lipid nanoparticles with iRGD peptide

SLNs were functionalized with iRGD peptide, through the maleimide thiol reaction. Namely, the conjugation of iRGD peptide onto preformed robust SLNs, based on the effortless binding between the thiol in iRGD peptide and the maleimide group on the SLNs surface. Briefly, 50 μL of

iRGD peptide (1 mg/mL) was added to 2 mL of the SLNs suspension and incubated for 1 h at room temperature. The pH of the reaction was kept between 6.5 and 7.5, to ensure that the maleimide reacted with the sulphridyl group of the peptide. The double bound of the maleimide reacted with the thiol group on the cysteine of the peptide to form a stable carbon–sulfur bond. The reaction resulted on the formation of a not reversible tioether bond. To remove the non-bonded peptide, the functionalized SLNs were carefully purified using centrifugal concentrators (Centrifugal Filter Units-Amicon Ultra 100 k) by ultrapure water at 4 °C, 3500 rpm for 15 min (5 times). Finally, they were stored at 4 °C.

2.5. Evaluation of drug encapsulation efficiency

The percentage of encapsulation efficiency (EE%) of PTX inside the SLNs were evaluated using the HPLC (Agilent 1 260, Agilent Technologies, USA). Shortly, 200 μL of SLNs were freeze-dried and after being dissolved with 1 mL acetonitrile, 20 μL of the resulting solution were injected into HPLC. For the HPLC detection was used a Discovery C_{18} column (15 cm × 4.6 mm, 5 μm) and the mobile phase consisted of water and acetonitrile (48:52) with detection at 227 nm. Drug encapsulation efficacy was calculated using Eq. (1):

$$EncapsulationEfficacy(\%) = \frac{WeightofdruginSLN}{Weightofdrugaddedinitially} \times 100 \quad (1)$$

2.6. Particle size, size distribution and surface charge

After preparation, the nanoparticles were characterized by dynamic light scattering to obtain information about their size, polydispersity index (PDI), and zeta (ζ)-potential, using Malvern Zetasizer Nano instrument (Malvern Ltd., UK). About 1 mL of a 1:100 dilutions of each sample with demineralized water, was pipetted into a disposable polystyrene cuvette (Sarstedt AG & Co., Germany) and the measurements were carried out at 25 ± 0.1 °C. The surface ζ-potential of the nanoparticles was measured by pipetting 750 μL of each particle suspension into a disposable folder capillary cell (DTS1070, Malvern, UK); all samples were redispersed in MillQ-water (pH 7.4) before assessing their surface potential. The results are shown as numeric average and standard deviation of the measurements of 3 different samples, each sample measured 3 times.

2.7. Estimation of peptide quantity on the solid lipid nanoparticles

iRGD with a fluorescein isothiocyanate (FITC) group was conjugated onto SLNs by the same reaction of iRGD-SLNs fabrication described above. Then, 1 mg/mL FITC-iRGD-SLNs were solubilized by 0.5% Triton-100 to ensure FITC was not being quenched and subjected to fluorescence detection. A standard curve of free FITC-iRGD was used to calculate the molar concentration of FITC-iRGD in SLNs samples.

2.8. In vitro drug release study

Studies of PTX release from SLNs were conducted using Franz cells (Lopedota et al. 2016), and experiments were performed in presence and absence of lipase from porcine in the donor compartment. Briefly, 500 μL of SLN-PTX was diluted with 500 μL of water or lipase (1 mg/mL in water) and placed on the diffusion barrier (area of 0.6 cm^2) constituted by an artificial cellulose acetate membrane (1 kDa, Fisher Scientific Milano), which divides donor and receptor cells. Phosphate buffer (PBS, 10 mM, pH 7.4) with 1% (w/v) of Tween 80 was chosen as receptor medium and it was constantly stirred and preserved at a temperature of (37 ± 0.5 °C). In an overall time of 72 h, 0.2 mL was picked up from the receiving compartment at set times, and to provide the sink conditions the equivalent volume of refreshing PBS was included in the receptor cell. The collected fractions were analyzed by HPLC to determine the drug content. Each experiment was performed in triplicate and was conducted in three separate Franz cells using three distinct batches of SLNs.

2.9. Stability studies

The assessment of the short-term stability of SLNs was verified by checking the size distribution of iRGD-SLNs in PBS (pH 7.4) and in DMEM supplemented with 10% (v/v) of FBS. The experiment was conducted at 37 °C by incubating 200 μL of iRGD-SLN in 1.5 mL of physiological relevant medium. At set times (5, 15, 30, 60, 90, and 120 min) a certain amount of sample was taken and diluted in water to assess the change in size over time. Triplicates of each experiment were performed.

2.10. Cell culture

Human glioblastoma U87-MG cells were purchased from American Type Culture Collection (ATCC, VA, USA) and were cultured as previously reported (Arduino et al. 2021).

For U87-MG tumour spheroids formation, cells were seeded at a density of 5000 cells per well on 96-wellplateCorning®Spheroid Microplate and incubated at 37 °C under 5% CO_2 for 5 days before performing experiments. Spheroid formation was assessed using OLYMPUS CKX41 microscope. (OLYMPUS, Tokyo, Japan)

2.11. In vitro cytotoxicity study

In order to perform the *in vitro* cytotoxicity study, U87-MG cells seeded in 96-well plates (PerkinElmer Inc., USA) at a density of 5000 cells per well wereleft attaching overnight before performing the assay. Afterward, cells were treated for 24 h at 37 °C with suspensions in DMEM of empty SLNs (SLN), PTX loaded SLNs (PTX-SLN) and of targeted PTX loaded SLNs (iRGD-PTX-SLN) at different concentrations in terms of nanoparticles (25, 50, 100, 250, 500 and 1000 μg/mL), and then washed out and cultured in fresh medium up to 72 h by the start of the experiment. Cells treated with solutions of free PTX at concentrations corresponding to those loaded in SLNs (0.275, 0.55, 1.1, 5.5, 11, 22 μg/mL) were used as reference. After that, the plates were equilibrated at room temperature for 30 min and the wells were washed once with 100 μL of HBSS–HEPES buffer. Then, 50 μL of Cell Titer-Glo (Promega Corporation, USA) were added to 50 μL of HBSS–HEPES (pH 7.4) in each well. The plates were stirred for 2 min on an orbital shaker and then stabilized for 30 min at room temperature, protected from the light. Finally, the luminescence was measured using a Victor TM X3 (WALLAC Oy,Turku, Finland by PerkinElmer Singapore) plate reader. The number of viable cells was quantified based on the amount of ATP produced by metabolically active cells. Data were plotted as % cell viability, normalized vs untreated cells, registered for each tested concentration.

2.12. In vitro uptake study on 2D and 3D model of glioblastoma

The internalization studies of the targeted iRGD-SLN were conducted *in vitro* both in 2D and 3D models of human glioblastoma U87-MG cells by means of flow cytometry analysis and fluorescence imaging. For these experiments, iRGD-functionalized and non-functionalized SLNs were loaded with the fluorescent dye BODIPY (BDP).

For the uptake experiment in 2D, according to a protocol described in Iacobazzi *et al.* (Iacobazzi et al. 2017), U87-MG cells were seeded in 6-well plates (Corning®) at a density of 300,000 cells per well and after attachment were incubated at 37 °C and at 4 °C (for external binding detection), for 2 h with the targeted iRGD-BDP-SLN and for comparison with the no targeted BDP-SLN, at a concentration of 0.01 μM in terms of the loaded fluorescent dye (BDP).Then, cells were maintained at 4 °C for the rest of the experiment, detached with trypsin-EDTA, washed with cold PBS, and finally re-suspended in PBS without Ca^{2+} and Mg^{2+}. The

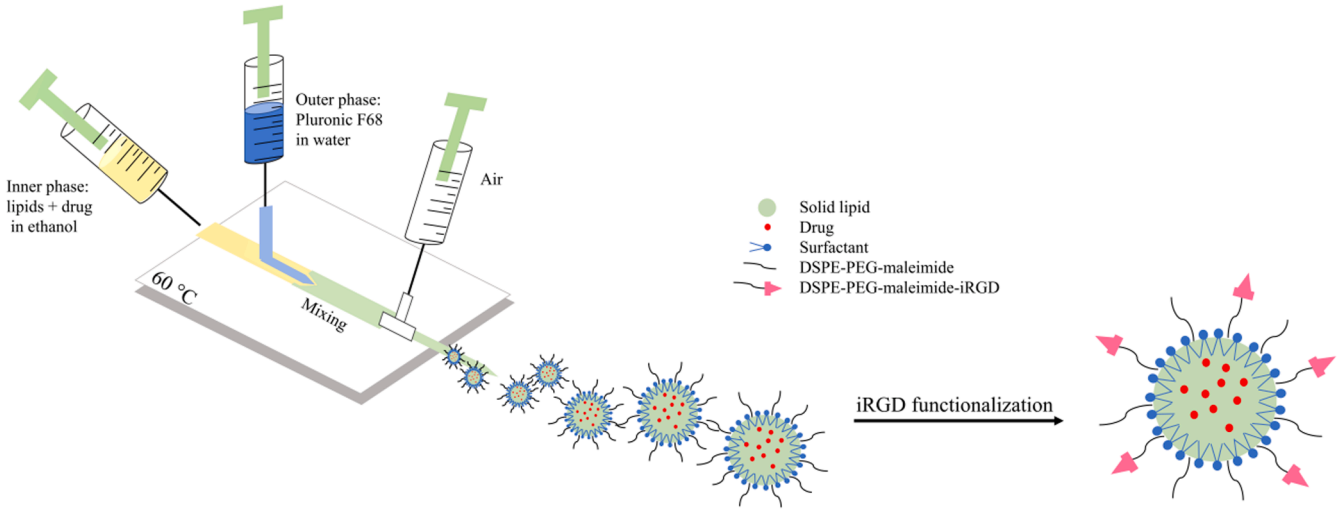

Fig. 1. Schematic representation of the setup for producing SLNs using microfluidics and later functionalisation.

cell-internalized fluorescence was measured by flow-cytometry on AttuneNxT acoustic focusing cytometer (Thermo Fisher Scientific, Waltham, MA, USA). 10,000 events were counted in the viable gate and the geometric mean of the viable cell population exposed to SLNs compounds was used to determine their internalization, after correction for cell auto-fluorescence and for SLNs compounds-autofluorescence. In particular, the amount of internalized SLNs was calculated substracting 4 °C values from 37 °C values. Data were interpreted using the Attune NxT Analysis Software (Thermo Fisher Scientific, Waltham, MA, USA) the CytExpert software v.1.2, provided by the manufacturer and represent mean ± SD, n = 3.

For the competition study, cells were pre-incubated for 30 min with excess of iRGD (5 μM) prior the addition of the targeted iRGD-BDP-SLN. After the incubation time, cells were processed as described above and the cell-associated fluorescence measured by flow-cytometry.

The qualitative analysis of the uptake was performed on 3D model of U87-MG cells allowed to generate spheroids on 96 well plate Corning®Spheroid Microplate for 5 days. After incubation for 2 h with iRGD-BDP-SLN and bare SLN-BDP and for 30 min with Hoechst 33,342 dye (2 μg/mL, InvitrogenTM) for nucleic acid staining, spheroids were washed and recovered with PBS without Ca^{2+} and Mg^{2+} and finally visualized on Celldiscoverer 7 microscope (Carl Zeiss Microscopy, Germany), with a Plam-Apochromat 20×/0.95 objective and optavar 0.5x tubelens. The competition study was also conducted in the 3D model, as described above.

2.13. Statistical analysis

Results were expressed as mean ± SD from three independent experiments. For cell viability test statistical significance was calculated using a two-way analysis of variance (ANOVA) followed by the Bonferroni post hoc tests (GraphPad Prism vers 5.0). For the uptake study *in vitro,* the significance was calculated using paired Students's *t*-test method (two-tailed). Statistically significant differences were set at probabilities of *p < 0.05, ** p < 0.01 and *** p < 0.001.“

3. Results and discussion

3.1. Preparation and characterization of solid lipid nanoparticles

The production of SLNs by microfluidics was carried out for the first time by our research group (Arduino et al. 2021). Through a process of optimisation of several parameters, the best conditions to produce SLNs with small size, narrow size distribution and good encapsulation efficiency were achieved. SLNs are produced in a single continuous step through a microfluidic chip based on glass capillaries. The use of microfluidics technology achieved high yield, good reproducibility, and precise control over the physical properties of SLNs, which are critical pre-conditions for its successful industrialization. In this work, SLNs loaded with PTX were produced by microfluidic technique and subsequently functionalised with the iRGD peptide (Fig. 1).

Table 1
Intensity-average hydrodynamic diameter and corresponding PdI determined by DLS, ζ-potential value, drug encapsulation efficiency (EE, %) of all prepared SLNs.

Nanoformulation	d_{mean} (nm)	Polydispersity index (PdI)	ζ-potential (mV)	Encapsulation Efficiency (EE%)
SLN	124.4 ± 2.7	0.155 ± 0.023	−36.8 ± 1.2	–
SLN-PTX	136.3 ± 3.1	0.101 ± 0.037	−31.1 ± 0.8	40.4 ± 6.8
SLN-BDP	133.3 ± 4.2	0.156 ± 0.044	−30.2 ± 2.3	29.3 ± 5.2
iRGD-SLN	142.7 ± 2.9	0.205 ± 0.020	−21.8 ± 1.9	–
iRGD-SLN-PTX	137.3 ± 2.5	0.279 ± 0.013	−11.2 ± 3.3	31.7 ± 4.8
iRGD-SLN-BDP	145.2 ± 5.8	0.221 ± 0.073	−12.4 ± 3.5	27.2 ± 2.2

Mean ± SD are reported, n = 3.

The SLNs were fully characterized, and the results are shown in Table 1. SLN-PTX presented an average size of 136.3 ± 3.1 nm and a PdI of 0.101 ± 0.03, whereas SLNs without PTX presented an average size of 124.4 ± 2.7 and a PdI of 0.155 ± 0.023. SLNs displayed narrow distribution range, which is indicated by a low PdI, the slight increase in size in SLN-PTX was ascribed to the PTX loaded within the nanosystem. Overall, a clear improvement in terms of homogeneity and reproducibility of the preparation emerged from the comparison of the properties of the SLNs obtained by microfluidics with respect to those obtained in bulk (data reported in (Arduino et al. 2021)).

Moreover, as shown in our previous work, to produce SLNs with a size around 100 nm the flow rate ratio employed was 1:5, demonstrating that an increase in the flow rate ratio resulted in an effective improvement in mixing (Arduino et al. 2021). In fact, as reported in the literature and in agreement with our work, the flow rate ratio influences the size of the nanoparticles (Jahn et al. 2010; Maeki et al. 2015). In addition, the size reduction was achieved by employing a microfluidic device

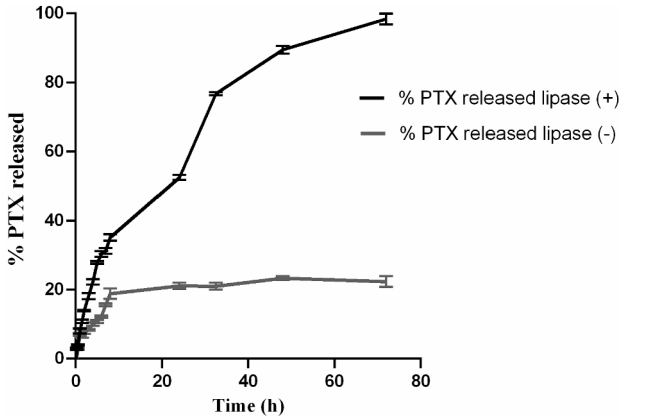

Fig. 2. In vitro release profiles of PTX from SLN in PBS at 37 °C. SLNs were diluted with water (% PTX released lipase (-)) or lipase (% PTX released lipase (+)) in the donor compartment. Results are reported as mean ± SD, n = 3.

connected to a three-port valve, which through a continuous pumping of air, improved the mixing (Arduino et al. 2021). The ζ-potential measurements highlighted the presence of an overall negative charge on the surface of all SLNs and provided values ranging from −11.2 to −36.8 mV. The bare SLNs obtained a ζ-potential value of − 36.8 ± 1.2 mV, similarly to the SLN-PTX that showed − 31.1 ± 0.8 mV. However, the ζ-potential of SLNs increased after conjugation with iRGD to − 21.8 ± 1.9 and − 11.2 ± 3.3 mV, respectively. This suggested that the functionalization of the SLNs with iRGD peptide occurred effectively, due to the decreased amount of maleimide groups on the SLNs' surface and the overall charge of the side chains of the peptide.

The SLNs were also prepared using a PEG modified phospholipid, which allowed the binding with iRGD peptide by its maleimide group, but also the function of reducing the opsonization of SLNs and the uptake by the endothelial reticular system (Arduino, Iacobazzi, et al. 2020). In particular, iRGD was conjugated to the maleimide group of DSPE-PEG-maleimide through maleimide-thiol reaction as already described (Wang et al. 2014; Yan et al. 2016). It is well documented in the literature that iRGD peptide can promote the penetration and tumour cell entry of a range of therapeutics in multiple cancer types (Liu et al. (2017c); McNeil 2016; Sugahara et al. 2010). For example, through the iRGD conjugation on 230 nm doxorubicin loaded liposomes, the authors successfully demonstrated facilitated cellular uptake of liposomes and an ~ 2-fold enhanced antitumor effect in a subcutaneous breast cancer (4 T1) model (Liu et al. 2013). Furthermore, Garanti*et al.* demonstrated the higher cell death and the greater uptake of the iRGD-SLNs toward U87 MG cells confirmed the potential of using this targeting strategy for the treatment of glioblastoma (Garanti et al. (2020)).

To estimate the concentration of peptide on the iRGD-SLNs, a fluorescent peptide FITC-iRGD was conjugated and the fluorescence of the resultant FITC-iRGD-SLNs was assessed. By comparison to a fluorescent standard curve of free FITC-iRGD, it was calculated that 1 mg/mL of iRGD-SLNs contained an average of 20 μM of peptide.

For all the SLNs, the EE (%) values represent the amount (*w/w*, %) of the drug incorporated in the lipid core of SLNs with respect to the starting drug amount employed for the preparation of lipid nanovectors. The good EE (%) values obtained were respectively 40.4 ± 6.8 % and 31.7 ± 4.8 % for SLN-PTX and iRGD-SLN-PTX, and confirmed the optimization of nanoparticles properties, including drugs encapsulation efficiency, due to the microfluidic assisted preparation.

In vitro drug release study was performed on SLN-PTX using Franz-diffusion cells at 37 °C in PBS (pH 7.4). As reported in the literature, SLNs are highly stable systems, and several studies have revealed that drug release from the lipid matrix occurs following degradation by enzymes in the cell (Arduino et al. (2020a), Arduino et al. (2020b)). The degradation velocity of SLNs depend on the nature of the lipid matrix, thus the *in vitro* release study, was conducted in presence of lipase in the donor compartment.

The drug release profiles shown in Fig. 2 indicated that PTX loaded SLNs exhibited sustained drug release behaviour. In the absence of lipase, SLNs released about 10% of PTX in 6 h, reaching 20% in 8 h maintaining this percentage until 24 h. Instead, in the presence of lipase, SLNs released about 35% of PTX in the first 6 h, 50% in 24 h and finally 100% in 72 h. The drug release kinetic properties that have emerged should be considered optimal in order to ensure a longer lasting controlled release of the drug at a specific site. This could not occur if PTX was not loaded into the drug delivery system. The SLNs appeared to have excellent colloidal stability without any sign of aggregation, as confirmed by the stability studies in Fig. 3 conducted for 2 h at 37 °C in PBS and cell culture medium.

3.2. Cell viability studies

The cell viability studies were performed on human glioblastoma U87-MG cells monolayer with a recovery from treatment protocol to assess the efficacy of the PTX formulated in the targeted nanoparticles system (iRGD-SLN-PTX) respect to PTX used as such. For comparison, no targeted SLN-PTX and the empty targeted iRGD-SLN were tested in order to verify both the advantage of formulating PTX in a selectively targeted system and the intrinsic toxicity of the carrier. As shown in Fig. 4, empty iRGD-SLNs were not cytotoxic in the range of concentrations explored, predicting that the antiproliferative effects induced by PTX-loaded-SLNs were not attributable to the carrier per se. As expected, PTX showed a concentration-dependent antiproliferative effect, although outperformed by that induced by iRGD-PTX-SLNs with cell viability values at the 11 μg/mL concentration in terms of PTX being 84 ± 6% and 67 ± 6%, respectively. In addition, iRGD-PTX-SLN also showed significantly higher toxicity than bare SLN-PTX (67 ± 6 % versus 77 ± 3 %), confirming the enhanced cytotoxic effect of targeted iRGD-PTX-SLN.

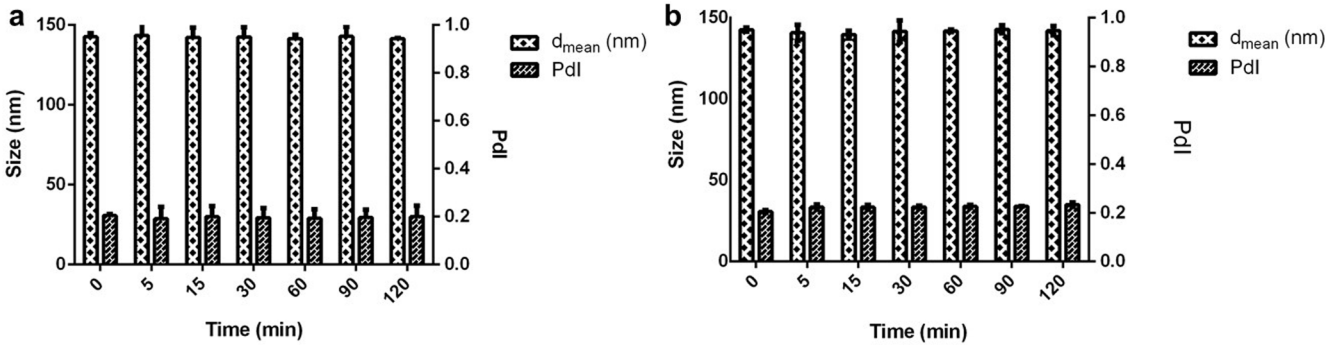

Fig. 3. Stability studies of iRGD-SLNs: hydrodynamic diameter and PdI index in (a) PBS (pH 7.4) and (b) cell medium at 37 °C after 2 h. Mean ± SD are reported, n = 3.

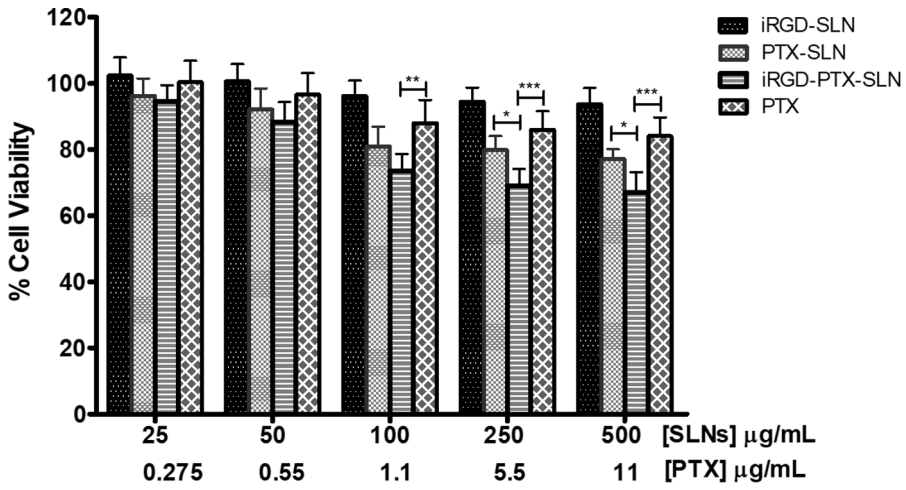

Fig. 4. Cell viability percentage of U87-MG cells as a function of the concentrations of SLN or PTX after 24 h incubation, followed by wash out and further 48 h of incubation in fresh culture medium.

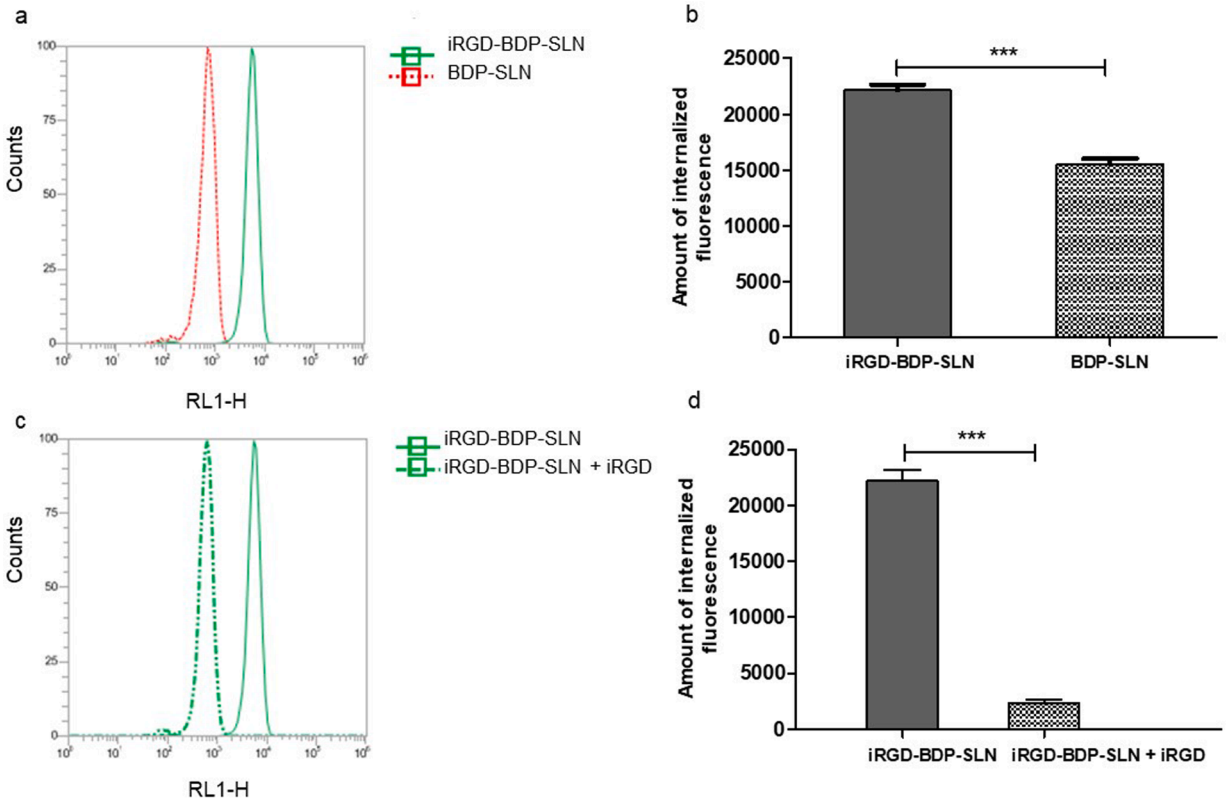

Fig. 5. Uptake studies of iRGD-SLN on 2D model of U87-MG cells. a) Flow cytometry histogram overlay for mean fluorescence value registered after incubation of U87-MG cells at 37 °C with iRGD-BDP-SLN (green continue line) or BDP-SLN (red dotted line); b) Amounts of internalized iRGD-BDP-SLN and BDP-SLN expressed as difference between mean fluorescence 37 °C and 4 °C registered values; c) Flow cytometry histogram overlay referred to the competition study: iRGD-BDP-SLN (green continue line), iRGD-BDP-SLN pre and co-incubated with iRGD (green dotted line); d) Amounts of internalized fluorescence registered after competition experiment with iRGD-BDP-SLN. (For interpretation of the references to colour in this figure legend, the reader is referred to the web version of this article.)

3.3. In vitro uptake study

The preferential uptake of the targeted iRGD-SLN into U87-MG cells overexpressing $\alpha_v\beta_3$ receptor (Garanti et al. (2020)) was quantitatively assessed by flow cytometric analysis conducted on U87-MG cells samples, obtained as described in the experimental section after incubation at 37 °C and 4 °C for 2 h with iRGD-BDP-SLN and for comparison with the bare-no targeted-BDP-SLN. Flow cytometry studies (Fig. 5 a,b) quantitatively confirmed that the introduction of iRGD targeting mojety induced an improvement in terms of amount of nanosystem and therefore of the drug, internalized by the cells. In fact, the amount of internalized fluorescence registered after the treatment with iRGD-BDP-SLN was significantly higher than with no-targeted-system-BDP-SLN (22160 ± 500 vs 15488 ± 550, respectively).). These results were explained by the involvement of the receptor-mediated uptake strategy for the internalization of the targeted SLNs and were corroborated by the competition study (Garanti et al. (2020)) (Fig. 5c, 5d). Infact, when cells were pre-incubated with iRGD before the addition of iRGD-BDP-SLN,

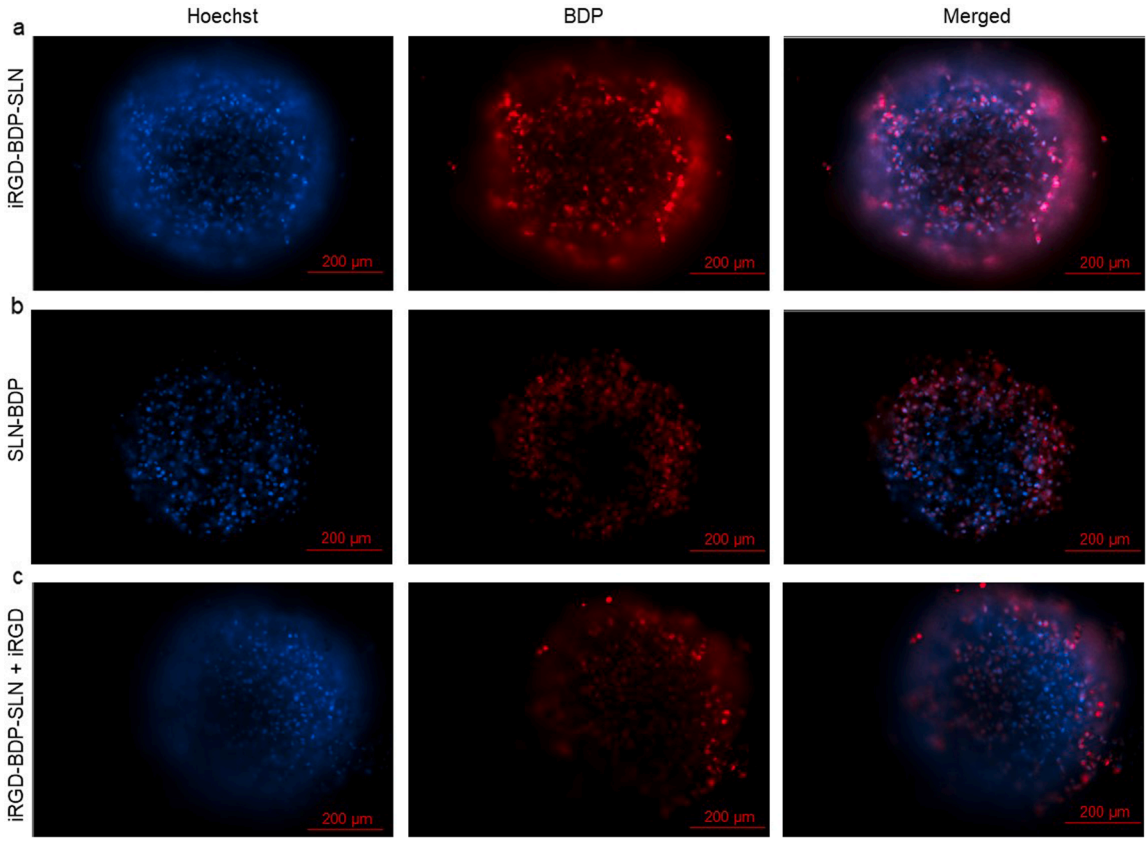

Fig. 6. Fluorescence uptake and competition imaging studies on 3D model of U87-MG cells. Panel a) show the fluorescence intensities of Hoechst (blue, nuclei), BDP (red, iRGD-BDP-SLN) and merge of them; Panel b) show the fluorescence intensities of Hoechst (blue, nuclei), BDP (red, BDP-SLN) and merge of them; Panel c) show the fluorescence intensities of Hoechst (blue, nuclei), BDP (red, iRGD-BDP-SLN + iRGD) and merge of them. Scale bar 200 µm. (For interpretation of the references to colour in this figure legend, the reader is referred to the web version of this article.)

the amount of internalized fluorescence was significantly lower (2352 ± 127 vs 22160 ± 500), confirming the effectiveness of the active targeting strategy pursued for SLN. These achievements agreed with the literature (Kuang et al. 2017), as Kuang et al. have demonstrated that c (RGDyK) decoration on the surface of SLNs could effectively enhance the cellular uptake of nanoparticles by U87MG cells. In the work Kuang verified that uptake of the SLNs was mediated through cRGD-receptor-dependent targeting, adding SLNs to cells pretreated with excess of free cRGD as competitive inhibition studies. As a result, green fluorescence was obviously decreased in that case.

Moreover, uptake and competition studies were conducted also on tumour spheroids of U87-MG cells to assess qualitatively the ability of iRGD-SLN to penetrate even a more complex structure than a 2D cell monolayer. It is acknowledged that experiments conducted on *in vitro* monolayer cellular model are not always the best way to demonstrate the activity of tumour drugs because it is necessary to consider the extracellular matrix and the microenvironment for tumour growth. Since spheroids may more closely mimic the characteristics of a solid tumour, the *in vitro* three-dimensional spheroid cell culture model was employed in this investigation (Nunes et al. 2019) (Sarisozen, Abouzeid, and Torchilin 2014). As clearly evidenced in the fluorescence imaging pictures the fluorescence intensity of iRGD-BDP-SLN (Fig. 6, panel a) displayed a more homogeneous intracellular localization throughout the spheroid, even in the core, as highlighted by the colocalization of the red signal related to the BDP-loaded nanoparticles with the Hoechst dye staining for nuclei, unlike the no target BDP-SLN, which appeared predominantly at the edges of the spheroids (Fig. 6, panel b).

Furthermore, the images related to the 3D competition study also confirmed a clear reduction of internalized fluorescence in the spheroid when it was pre-incubated and co-incubated with iRGD in addition to the iRGD-BDP-SLN (Fig. 6, panel c).

Fluorescence imaging investigation was consistent with FCM analysis to demonstrate the efficacy of active targeting to promote increased cell internalization.

4. Conclusions

In this work, the microfluidic technique was used to produce SLNs. The production of iRGD-functionalized SLNs by microfluidics is reported for the first time. Here we showed the parameters to manufacture SLNs and their later functionalization with the iRGD peptide. iRGD-SLN have enhanced the anticancer activity of PTX by increasing cytotoxicity and providing more efficient tumour targeting and penetration both in 2D and 3D models U87-MG cells. Overall, these results demonstrate that the surface functionalization of SLNs with iRGD improves cellular uptake and cytotoxicity ability. Furthermore, the investigated antitumor effects detected with the iRGD-SLN might also be potentially employed to other forms of cancers where integrin is associated.

CRediT authorship contribution statement

Ilaria Arduino: Methodology, Writing – original draft, Writing – review & editing. **Zehua Liu:** Methodology, Validation, Writing – original draft. **Rosa Maria Iacobazzi:** Methodology, Validation. **Angela Assunta Lopedota:** Formal analysis, Validation. **Antonio Lopalco:** Resources. **Annalisa Cutrignelli:** Investigation. **Valentino Laquintana:** Formal analysis, Validation. **Letizia Porcelli:** Resources. **Amalia Azzariti:** Data curation, Investigation. **Massimo Franco:** Data curation. **Hélder A. Santos:** Writing – review & editing, Supervision, Project administration. **Nunzio Denora:** Writing – review & editing,

Supervision, Project administration.

Declaration of Competing Interest

The authors declare that they have no known competing financial interests or personal relationships that could have appeared to influence the work reported in this paper.

Acknowledgements

H. A. S. acknowledges HiLIFE Research Funds, the Sigrid Jusélius Foundation, and the Academy of Finland (Grants No. 317042 and 331151)) for financial support.

References

Arduino, I., Iacobazzi, R.M., Riganti, C., Lopedota, A.A., Perrone, M.G., Lopalco, A., Cutrignelli, A., Cantore, M., Laquintana, V., Franco, M., Colabufo, N.A., Luurtsema, G., Contino, M., Denora, N., 2020a. Induced expression of P-gp and BCRP transporters on brain endothelial cells using transferrin functionalized nanostructured lipid carriers: A first step of a potential strategy for the treatment of Alzheimer's disease. Int. J. Pharm. 591, 120011.

Arduino, I., Liu, Z., Rahikkala, A., Figueiredo, P., Correia, A., Cutrignelli, A., Denora, N., Santos, H.A., 2021. Preparation of cetyl palmitate-based PEGylated solid lipid nanoparticles by microfluidic technique. Acta Biomater. 121, 566–578.

Arduino, I., Depalo, N., Re, F., Dal Magro, R., Panniello, A., Margiotta, N., Fanizza, E., Lopalco, A., Laquintana, V., Cutrignelli, A., Lopedota, A.A., Franco, M., Denora, N., 2020b. PEGylated solid lipid nanoparticles for brain delivery of lipophilic kiteplatin Pt(IV) prodrugs: An in vitro study. Int. J. Pharm. 583, 119351.

Peres, B., Luana, L.B., Peres, P.H., de Araújo, H., Sayer, C., 2016. Solid lipid nanoparticles for encapsulation of hydrophilic drugs by an organic solvent free double emulsion technique. Colloids Surf., B 140, 317–323.

Costa, C., Liu, Z., Martins, J.P., Correia, A., Figueiredo, P., Rahikkala, A., Li, W., Seitsonen, J., Ruokolainen, J., Hirvonen, S.-P., Ana Aguiar-Ricardo, M., Corvo, L., Santos, H.A., 2020. All-in-one microfluidic assembly of insulin-loaded pH-responsive nano-in-microparticles for oral insulin delivery. Biomater. Sci. 8, 3270–3277.

Costa, C., Liu, Z., Simões, S.I., Correia, A., Rahikkala, A., Seitsonen, J., Ruokolainen, J., Aguiar-Ricardo, A., Santos, H.A., Luísa Corvo, M., 2021. One-step microfluidics production of enzyme-loaded liposomes for the treatment of inflammatory diseases. Colloids Surf., B 199, 111556.

Garanti, T., Alhnan, M.A., Wan, K.-W., 2020. RGD-decorated solid lipid nanoparticles enhance tumor targeting, penetration and anticancer effect of asiatic acid. Nanomedicine 15.

Hussain, M.T., Tiboni, M., Perrie, Y., Casettari, L., 2020. Microfluidic production of protein loaded chimeric stealth liposomes. Int. J. Pharm. 590, 119955.

Iacobazzi, R.M., Porcelli, L., Lopedota, A.A., Laquintana, V., Lopalco, A., Cutrignelli, A., Altamura, E., Di Fonte, R., Azzariti, A., Franco, M., Denora, N., 2017. Targeting human liver cancer cells with lactobionic acid-G(4)-PAMAM-FITC sorafenib loaded dendrimers. Int. J. Pharm. 528, 485–497.

Jahn, A., Stavis, S.M., Hong, J.S., Vreeland, W.N., DeVoe, D.L., Gaitan, M., 2010. Microfluidic Mixing and the Formation of Nanoscale Lipid Vesicles. ACS Nano 4, 2077–2087.

Kuang, Y.e., Zhang, K., Cao, Y.i., Chen, X., Wang, K., Liu, M., Pei, R., 2017. Hydrophobic IR-780 Dye Encapsulated in cRGD-Conjugated Solid Lipid Nanoparticles for NIR Imaging-Guided Photothermal Therapy. ACS Appl. Mater. Interfaces 9, 12217–12226.

Liu, D., Zhang, H., Cito, S., Fan, J., Mäkilä, E., Salonen, J., Hirvonen, J., Sikanen, T.M., Weitz, D.A., Santos, H.A., 2017a. Core/Shell Nanocomposites Produced by Superfast Sequential Microfluidic Nanoprecipitation. Nano Lett. 17, 606–614.

Liu, D., Zhang, H., Fontana, F., Hirvonen, J.T., Santos, H.A., 2017b. Microfluidic-assisted fabrication of carriers for controlled drug delivery. Lab Chip 17, 1856–1883.

Liu, X., Jiang, J., Ji, Y., Jianqin, L.u., Chan, R., Meng, H., 2017c. Targeted drug delivery using iRGD peptide for solid cancer treatment. Mol. Syst. Des. Eng. 2, 370–379.

Liu, Y., Ji, M., Wong, M.K., Joo, K.-I., Wang, P., 2013. Enhanced Therapeutic Efficacy of iRGD-Conjugated Crosslinked Multilayer Liposomes for Drug Delivery. Biomed Res. Int. 2013, 378380.

Liu, Z., Fontana, F., Python, A., Hirvonen, J.T., Santos, H.A., 2020. Microfluidics for Production of Particles: Mechanism, Methodology, and Applications. Small 16, 1904673.

Lopedota, A., Cutrignelli, A., Laquintana, V., Denora, N., Iacobazzi, R.M., Perrone, M., Fanizza, E., Mastrodonato, M., Mentino, D., Lopalco, A., Depalo, N., Franco, M., 2016. Spray Dried Chitosan Microparticles for Intravesical Delivery of Celecoxib: Preparation and Characterization. Pharm. Res. 33, 2195–2208.

Lu, L.u., Zhao, X., Tiwei, F.u., Li, K.e., He, Y.e., Luo, Z., Dai, L., Zeng, R., Cai, K., 2020. An iRGD-conjugated prodrug micelle with blood-brain-barrier penetrability for anti-glioma therapy. Biomaterials 230, 119666.

Maeki, M., Saito, T., Sato, Y., Yasui, T., Kaji, N., Ishida, A., Tani, H., Baba, Y., Harashima, H., Tokeshi, M., 2015. A strategy for synthesis of lipid nanoparticles using microfluidic devices with a mixer structure. RSC Adv. 5, 46181–46185.

Martins, C., Araújo, F., Gomes, M.J., Fernandes, C., Nunes, R., Li, W., Santos, H.A., Borges, F., Sarmento, B., 2019. Using microfluidic platforms to develop CNS-targeted polymeric nanoparticles for HIV therapy. Eur. J. Pharm. Biopharm. 138, 111–124.

Martins, J.P., Torrieri, G., Santos, H.A., 2018. The importance of microfluidics for the preparation of nanoparticles as advanced drug delivery systems. Expert Opin Drug Deliv 15, 469–479.

McNeil, S.E., 2016. Evaluation of nanomedicines: stick to the basics. Nat. Rev. Mater. 1, 16073.

Nunes, A.S., Barros, A.S., Costa, E.C., Moreira, A.F., Correia, I.J., 2019. 3D tumor spheroids as in vitro models to mimic in vivo human solid tumors resistance to therapeutic drugs. Biotechnol. Bioeng. 116, 206–226.

Paliwal, R., Paliwal, S.R., Kenwat, R., Kurmi, B.D., Sahu, M.K., 2020. Solid lipid nanoparticles: a review on recent perspectives and patents. Expert Opin. Ther. Pat. 30, 179–194.

Ruoslahti, E., Pierschbacher, M.D., 1987. New perspectives in cell adhesion: RGD and integrins. Science 238, 491–497.

Sarisozen, C., Abouzeid, A.H., Torchilin, V.P., 2014. The effect of co-delivery of paclitaxel and curcumin by transferrin-targeted PEG-PE-based mixed micelles on resistant ovarian cancer in 3-D spheroids and in vivo tumors. Eur. J. Pharm. Biopharm. 88, 539–550.

Sugahara, K.N., Teesalu, T., Karmali, P.P., Kotamraju, V.R., Agemy, L., Girard, O.M., Hanahan, D., Mattrey, R.F., Ruoslahti, E., 2009. Tissue-penetrating delivery of compounds and nanoparticles into tumors. Cancer Cell 16, 510–520.

Sugahara, K.N., Teesalu, T., Karmali, P.P., Kotamraju, V.R., Agemy, L., Greenwald, D.R., Ruoslahti, E., 2010. Coadministration of a tumor-penetrating peptide enhances the efficacy of cancer drugs. Science 328, 1031–1035.

Tahir, N., Madni, A., Li, W., Correia, A., Khan, M.M., Rahim, M.A., Santos, H.A., 2020. Microfluidic fabrication and characterization of Sorafenib-loaded lipid-polymer hybrid nanoparticles for controlled drug delivery. Int. J. Pharm. 581, 119275.

Wang, K., Zhang, X., Liu, Y., Liu, C., Jiang, B., Jiang, Y., 2014. Tumor penetrability and anti-angiogenesis using iRGD-mediated delivery of doxorubicin-polymer conjugates. Biomaterials 35, 8735–8747.

Yan, F., Wu, H., Liu, H., Deng, Z., Liu, H., Duan, W., Liu, X., Zheng, H., 2016. Molecular imaging-guided photothermal/photodynamic therapy against tumor by iRGD-modified indocyanine green nanoparticles. J. Control. Release 224, 217–228.

Zheng, J., Wan, Y., Elhissi, A., Zhang, Z., Sun, X., 2014. Targeted paclitaxel delivery to tumors using cleavable PEG-conjugated solid lipid nanoparticles. Pharm. Res. 31, 2220–2233.